Machine Learning Algorithms for Breast Cancer Detection in Mammography Images: A Comparative Study

Rhaylander Mendes de Miranda Almeida[1], Dehua Chen[2], Agnaldo Lopes da Silva Filho[3] and Wladmir Cardoso Brandão[1][a]

[1]*Department of Computer Science, Pontifical Catholic University of Minas Gerais (PUC Minas), Belo Horizonte, Brazil*

[2]*Department of Computer Science, Federal University of Minas Gerais (UFMG), Belo Horizonte, Brazil*

[3]*Faculty of Medicine, Federal University of Minas Gerais (UFMG), Belo Horizonte, Brazil*

Keywords: Deep Learning, Classification, Mammography Screening, Mammogram Abnormalities, Breast Cancer.

Abstract: Breast tumor is the most common type of cancer in women worldwide, representing approximately 12% of reported new cases and 6.5% of cancer deaths in 2018. Mammography screening are extremely important for early detection of breast cancer. The assessment of mammograms is a complex task with significant variability due to professional experience and human errors, an opportunity for assisting tools to improve both reliability and accuracy. The usage of deep learning in medical image analysis have increased, assisting specialists in early detection, diagnosis, treatment or prognosis of diseases. In this article, we compare the performance of XGBoost and VGG16 in the task of breast cancer detection by using digital mammograms from CBIS-DDSM dataset. In addition, we perform a comparison of prediction accuracy between full mammogram images and patches extracted from original images based on ROI annotated by experts. Moreover, we also perform experiments with transfer learning and data augmentation to exploit data diversity, and the ability to extract features and learn from raw unprocessed data. Experimental results show that XGBoost achieves 68.29% in AUC, while VGG16 achieves approximately the same performance of 68.24% in AUC.

1 INTRODUCTION

According to the World Health Organization (WHO)[1] breast cancer is the most common cancer in women worldwide, causing more than 627 thousand deaths in 2018. The American Cancer Society estimated more than 41 thousand deaths and 268 thousand new cases of female breast cancer in the United States in 2019 (DeSantis et al., 2019). Mammography screening for early breast cancer detection has been adopted in many countries, helping in a significant reduction of deaths due to early diagnosis and treatment. While the benefits of mammography screening have been observed in the past years, its harms are also topics of discussion. For instance, overdiagnosis of breast cancer is the main harm resulted of mammography screening, with an estimated occurrence of 31% in the United States (Løberg et al., 2015).

Overdiagnosis is the diagnosis that would not have been identified clinically, but that is previously identified (Løberg et al., 2015). Tumor regression, lack of potential progression or even deaths caused by other reasons prior to the clinical surface are cases of overdiagnosis, all situations where the actual treatment will not have benefit (Løberg et al., 2015). Surgery, chemotherapy, antiestrogen treatment and radiotherapy are treatment options for breast cancer, and the last is known to increase the risk of death from cardiovascular disease (Løberg et al., 2015). While the risk of radiation exposure in a mammogram is small, the scenario may be different due to repeated X-rays in follow-up exams and considerably increased in cases of overtreatment (Darby et al., 2013).

The assessment of screening mammograms is a complex task which has significant variability due to many reasons such as professional experience and human errors. Therefore, it is encouraged the usage of Computer Aided Diagnosis (CAD) to aid radiologists in diagnosing cancer to improve reliability and accuracy (Ribli et al., 2018). Even though the quality of digital mammograms is higher when compared to the conventional film version, interpretation is still an issue as observer error is frequent in breast can-

[a] https://orcid.org/0000-0002-1523-1616

[1] http://www.who.int

Almeida, R., Chen, D., Filho, A. and Brandão, W.
Machine Learning Algorithms for Breast Cancer Detection in Mammography Images: A Comparative Study.
DOI: 10.5220/0010440906600667
In *Proceedings of the 23rd International Conference on Enterprise Information Systems (ICEIS 2021) - Volume 1*, pages 660-667
ISBN: 978-989-758-509-8

cer screening, leading to misinterpretations of abnormalities or even lack of identification (Vadivel and Surendiran, 2013). Abnormalities found in a mammogram are broadly categorized as masses and calcification, which have several distinguishing characteristics used to classify a mammogram as benign or malignant (Vadivel and Surendiran, 2013). Due to the high correlation between breast cancer and the appearance of abnormalities, along with the difficulty in distinguishing some characteristics such as shape and margin, the use of CAD to help radiologists in abnormality classification represents an opportunity to reduce misdiagnosis (Vadivel and Surendiran, 2013).

The use of Machine Learning (ML) have increased in several research areas due to the increase of the computing power required to train effective models, and the increase in the availability and capacity of processing big amounts of data in the learning process (Shen et al., 2017). The ability of learning from raw and unlabeled data and the capacity of addressing complex problems and data structures are also key factors to the increase on usage of ML (Bakator and Radosav, 2018). Remarkable results have been achieved by Deep Learning (DL) models in medical image analysis to support specialists in early detection, diagnosis, treatment or prognosis of diseases (Shen et al., 2017), which is expected to increase the overall quality of healthcare (Bakator and Radosav, 2018). The accuracy and reliability of mammography assessment vary with the level of expertise of each specialist and a high variability has been observed in previous studies (Sprague et al., 2016). Hence, this represents an opportunity for the application of CAD for mammography assessment to achieve reliable and accurate solutions based on DL models.

In this article, we compare the performance of XGBoost, a classic tree-based ML algorithm and VGG16, a Convolutional Neural Network (CNN), in the task of breast cancer detection using the Curated Breast Imaging Subset of DDSM (CBIS-DDSM) dataset composed of full mammogram images and abnormality-focused patches extracted from original images properly labeled by a trained mammographer (Lee et al., 2017). In particular, XGBoost is a scalable gradient boosting library designed to handle big amounts of data while consuming fewer resources (Chen and Guestrin, 2016), while VGG16 is one of the famous CNN architectures proposed during the 2014 ImageNet (Simonyan and Zisserman, 2014; Russakovsky et al., 2015). We also compare the ability of the algorithms to extract features and learn from raw data.

The remainder of this article is organized as follows. In Section 2, we present a literature review. In Section 3 we present relevant related work reported in literature. Section 4 describes our proposed approach to perform breast cancer detection, comparing ML algorithms. In Section 5 we present the experimental setup. Section 6 presents the experimental results. Finally, in Section 7 we present the conclusion and directions for future work.

2 BACKGROUND

Machine Learning systems are able to learn from past experiences to make decisions with no need of explicit instructions. The learning process is based on inductive reasoning, in which generic conclusions are reached based on a dataset (Russell and Norvig, 2009). ML models are created based on datasets with examples from the problem domain. However, datasets often present imperfections, such as inconsistency, redundancy, missing and noisy data. Hence, ML algorithms must be robust to minimize the impact of data imperfections. Data preprocessing is usually required to reduce this impact and improve generalization.

Particularly, the goal is to find a ML model with good generalization, being capable of accurately predict not only the training data but also unknown data from the problem domain. Bad generalization might be a result of overfitting, when a model performs well on the training data but has poor generalization on new data items, or underfitting, when a model does not perform well on the training data and has poor generalization on new data items (Russell and Norvig, 2009).

There are different ML algorithms reported in the literature. Decision trees use the divide and conquer strategy to solve complex problems by recursively splitting them into smaller ones. The data space is split on each recursive interaction based on feature values. Branches are created every time the data space is split and a decision rule is defined to describe a portion of the data space. A tree model is either defined as classification tree if the target variable is a finite set of values, or as regression tree if the target variable can take continuous values.

Boosting algorithms combine weak learners into an ensemble, resulting in a strong learner. A weak learner is a classifier slightly better than a random pick, and a strong learner is a well-correlated arbitrary classifier with lower error rate. The main idea is to interactively associate a hypothesis and a weight to each example of the training set so that the classification may focus on different examples leading to different classifiers. On each interaction

the weights are adjusted and a weak classifier is incorporated. The ensemble output is the result of a weighted vote of all classifiers. Gradient boosting is commonly used with decision trees and has proven to be effective and widely used on many ML challenges (Chen and Guestrin, 2016). Extreme Gradient Boosting (XGBoost) is a scalable gradient boosting library designed to handle billions of examples by providing a parallel tree boosting that consume fewer resources, while achieving state-of-the-art performance (Chen and Guestrin, 2016).

An Artificial Neural Network (ANN) is a distributed system composed of simple processing units connected together, which have the ability to learn from the environment and preserve experimental knowledge (Russell and Norvig, 2009). The development of ANNs is inspired by the human's nervous system and aimed the creation of models with similar learning capabilities of the human brain to acquire knowledge. High generalization, fault tolerant, robustness to deal with noisy raw data are reasons for ANNs popularity. However, the decisions taken by their complex mathematical (black box) models are usually difficult to understand. Thus "white box" systems are generally preferred by industries, since their results are easily interpretable by humans (Loyola-González, 2019).

Deep Learning (DL) is used to describe ANNs with complex multilayers architecture (Liu et al., 2017; Abiodun et al., 2018). By simulating how key sensory areas of the human brain work (Pouyanfar et al., 2018), DL models can represent complex structures and are able to automatically perform feature extraction (Abiodun et al., 2018). They require large datasets for training to effectively prevent overfitting (Liu et al., 2017). Particularly, remarkable results have been achieved by DN in the medical field to support specialists in early detection, diagnosis, treatment and prognosis of diseases (Shen et al., 2017). The ability of learning from unlabeled raw data to automatically identify abstractions brings a lot of value in the medical field (Bakator and Radosav, 2018). Tissue segmentation, structure detection, computer-aided disease diagnosis and prognosis are specific uses of DL in the medical field (Shen et al., 2017; Bakator and Radosav, 2018).

Convolutional Neural Network (CNN) is a popular DL architecture extensively used in computer vision, audio and speech processing, and natural language processing (Pouyanfar et al., 2018; Abiodun et al., 2018). Recently, an effective CNN model called VGG16, achieves high accuracy on image classification (Simonyan and Zisserman, 2014). In particular, VGG16 is a VGGNet with 16 layers that uses smaller (3x3) convolution filters stacked together producing deeper networks with the same effective receptive field and capable of handling more non-linearities, and fewer parameters (Simonyan and Zisserman, 2014).

3 RELATED WORK

DL models have been extensively used in medical image analysis achieving remarkable results(Shen et al., 2017; Bakator and Radosav, 2018). A CNN model performs breast density classification based on the four BI-RADS classes, using a dataset of over 200,000 screening mammography exams(Wu et al., 2018). Particularly, it uses pixel intensity as a baseline, since fibroglandular tissue absorbs much of the radiation, which make them appear brighter than adipose tissue. The authors report accuracy similar to human experts. In the same vein, a similar CNN-based classifier based on AlexNet model can consistently distinguish between the difficult classes "scattered areas of fibroglandular density" and "heterogeneously dense" (Mohamed et al., 2018).

A challenging problem in DL for medical image analysis is the access to large datasets with reliable annotations from domain experts (Tan et al., 2018). Transfer learning can mitigate this problem by training a model in a source domain with high quality data, later using the learned model to perform predictions in a target domain(Tan et al., 2018; Perre et al., 2019). In the context of lesion classification in mammograms, transfer learning was already been effectively used to overcome the problem of missing datasets (Perre et al., 2019).

Experiments reported from the Digital Mammography DREAM Challenge (DM Challenge) to diagnosis breast cancer using a dataset with 86,000 exams show that an ensemble of two CNN models (R-CNN and VGG16) can effectively detect breast cancer in mammography (Ribli et al., 2018). Additionally, other different DL architectures present outstanding performance for the same task (Li et al., 2019). Moreover, random trees and random forest have also been used to classify mammograms and the authors reported 90% of accuracy (Vibha et al., 2006).

4 METHODOLOGY

As mentioned in the Section 2, DL can represent complex models, automatically performing feature extraction learning from raw data (Abiodun et al., 2018;

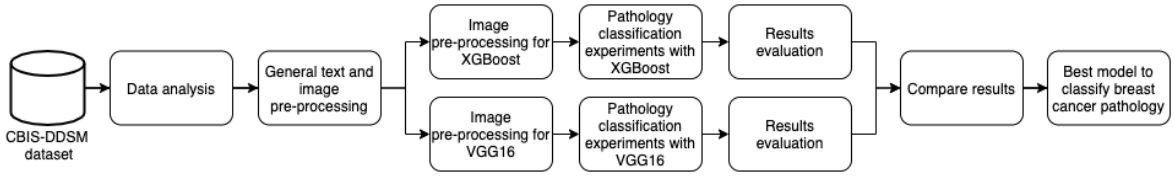

Figure 1: The methodology used to compare different algorithms for breast cancer detection.

Pouyanfar et al., 2018). In this article, we compare the performance of the traditional XGBoost algorithm and the classic VGG16 DL network for breast cancer pathology classification on raw mammogram images available in the CBIS-DDSM dataset.

Figure 1 presents each step of the comparison methodology. First, we perform an analysis of the dataset to understand available data and how it can be used for breast cancer detection. Second, general pre-processing steps are performed to fix and enhance text metadata available in the dataset and extract raw image data from DICOM files, creating intermediate datasets. Third, different experiments are carried out using both XGBoost and VGG16 to perform pathology classification in mammograms. Particularly, each ML algorithm requires specific image pre-processing steps to adjust the dataset to the expected input format and to perform data augmentation. Fourth, experimental results are collected and compared based on research questions made on each experiment. Finally, the most effective model of each ML algorithm are evaluated and compared. The AUC metric and confusion matrix are used to compare the results obtained by the classification models.

5 EXPERIMENTAL SETUP

5.1 Dataset

The Curated Breast Imaging Subset of DDSM (CBIS-DDSM) dataset is composed of decompressed DICOM images selected and curated by specialists (Lee et al., 2017). It contains 10,239 images of 6,775 cases from 1,566 patients, 753 of them calcification cases, and other 891 mass cases. Table 1 presents the number of images tagged as benign or malignant in CBIS-DDSM by category.

Each patch extracted from mammograms has an equivalent ROI segmentation filter. The 3,568 ROI filters are not relevant to this work, so from the original 10,239 images we removed 3,568, considering only 6,671 images. There is no standard resolution across all images in the dataset. Usually mammograms have resolutions higher than 3000x4000 pixels, and the resolution of ROI patch images presents high variability, ranging from 100x100 up to 2000x2000 pixels.

Table 1: Number of images by category in CBIS-DDSM dataset.

	Train		Test		
Category	Ben.	Mal.	Ben.	Mal.	Total
Mammograms	1,354	1,104	385	260	3,103
ROI patches	1,683	1,181	428	276	3,568
Total	3,037	2,285	813	536	6,671

Each case contains the original decompressed images of Medio-Lateral Oblique (MLO) and Cranial-Caudal (CC) views of mammograms from both breasts, a ROI segmentation filter, patches containing ROI for each abnormally found on each mammogram image, and metadata information about the patient (Lee et al., 2017). The available information on patient are: Breast Imaging Reporting and Data System (BI-RADS) classification for mass shape, mass margin, calcification type, calcification distribution, and breast density, overall BI-RADS assessment from 0 to 5, rating of the subtlety of the abnormality from 1 to 5, age, date of the study, date of digitization, dense tissue category, scanner used to digitize, resolution of each image, and pathology (Lee et al., 2017). Figure 2 shows different examples of images available in the dataset, CC, MLO, and ROI patch images from both benign and malignant abnormalities are visible for calcifications (a) and masses (b).

5.2 Data Pre-processing

5.2.1 Metadata Files

As mentioned in the Section 5.1, the dataset not only has DICOM images but also metadata files. In particular, there are three columns used to map the path to patients' original decompressed images, ROI segmentation filter and bounding boxes of all abnormalities found on each original image. However, the paths were all broken as the inner folder names were all incorrect. Once this scenario was identified as part of the dataset analysis, the first pre-processing effort was to fix all paths and create two additional types of metadata files after separating original mammograms and patch images. The latter was required as

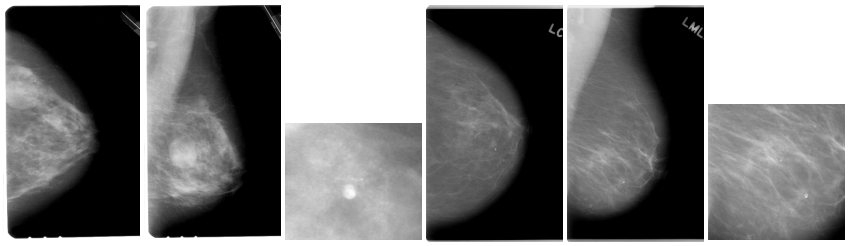

(I) CC (II) MLO (III) ROI patch (IV) CC (V) MLO (VI) ROI patch

(a) Examples of benign (I, II, and III) and malignant (IV, V, and VI) calcifications, they belong to a single breast of two randomly picked patients.

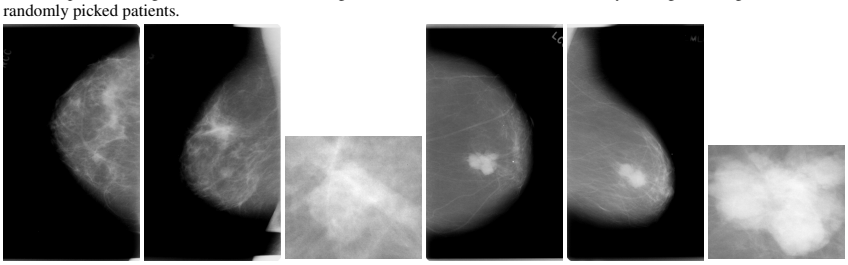

(I) CC (II) MLO (III) ROI patch (IV) CC (V) MLO (VI) ROI patch

(b) Examples of benign (I, II, and III) and malignant (IV, V, and VI) masses, they belong to a single breast of two randomly picked patients.

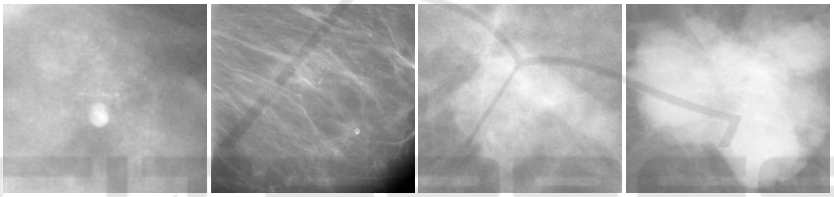

(I) Benign (II) Malignant (III) Benign (IV) Malignant

(c) Examples of benign and malignant abnormalities, calcifications (I, II) and masses (III, IV).

Figure 2: Example of images from CBIS-DDSM dataset.

each metadata file would have duplicated instances in case a mammogram would have multiple abnormalities. This approach made it easier to perform further experiments based on image types. Manual human verification was required in order to ensure all image paths were correct, a script to create thumbnails was created to facilitate this effort.

5.2.2 Images

All experiments have been performed using raw images. Data augmentation techniques were used to increase the data diversity of the dataset for training and as a mechanism to help dealing with overfitting. Images were generated during execution time, and the number of images is the same as the number of original images in the dataset. The random transformations performed as part of data augmentation are random horizontal flips, rotation around the center, shear transformation, vertical and horizontal shifts, and zoom in and out. Lastly, images are resized to 224x224 pixels to comply with VGG16's input and to reduce data dimensionality.

Since all images from the dataset are in the DICOM format, the pixel data information is extracted and stored as TIFF format. During this step three datasets are created, one containing only original mammograms, another for abnormality patches and the last one containing both image types, respectively called dataset A, B and C, as presented in Table 2. These datasets are used individually to evaluate and compare how models perform when using raw original images versus focused abnormality patches extracted from original images, and to evaluate if mixing them would bring any benefits.

Table 2: Datasets created after grouping images by category.

	Train		Test		
Dataset	Ben.	Mal.	Ben.	Mal.	Total
A	1,354	1,104	385	260	3,103
B	1,683	1,181	428	276	3,568
C	3,037	2,285	813	536	6,671

5.3 Training and Validation

As mentioned in Section 5.2.2, we use data augmentation to perform random transformations on images during the training phase to not only increase data diversity, but also to reduce overfitting. The images used for validation are not transformed, except for resizing all of them to keep the same dimensions. Knowledge transfer and fine-tuning have been used for both XGBoost and VGG16 models. Additionally, the three datasets mentioned in Table 2 have been used individually and also combined for transfer learning as described in Section 6. We use AUC to measure model's performance for classifying patient's pathology. We also present Confusion Matrix to improve understanding in which class the models performs better (or worst).

For XGBoost, we use 5-fold cross-validation for tuning and Grid Search to find hyperparameters, in particular *learning rate* = *0.2*, *gamma* = 1.5, *max tree depth* = 5, *min child weight* = 3 and *subsample* = 0.8. In addition, to avoid overfitting we set *epoch limit* to 30. For VGG16, we use the last fully softmax connected layer to properly classify outputs in two classes. In addition, knowledge transfer has been used by loading weights from ImageNet VGG16 ILSVRC2014 (Russakovsky et al., 2015) to understand if the learned knowledge is useful for breast pathology classification. For fine-tuning, we test three different models: load weights from ImageNet VGG16 ILSVRC2014 while locking convolutional layers, training only the last max pooling and fully connected layers; use the previous models as a starting point, but unlocking convolutional layers; train the entire network from scratch. For all the models the training upper limit of epochs was set to 100 and an early stopping callback was leveraged to stop the execution in case there was no improvement in AUC metric during the course of 30 consecutive epochs. An stochastic gradient descent (SGD) optimizer was used with *learning rate* = 1e-4 and *momentum* = 0.9.

6 EXPERIMENTAL RESULTS

In this section, we present the experiments we carried out to evaluate the performance of XGBoost and VGG16 in the task of breast cancer detection using mammograms. As mentioned in the Section 5.1, since the CBIS-DDSM dataset has full mammogram images and abnormality-focused patches extracted from the original images, three other datasets were created during pre-processing as an effort to have control over an image type used as input and to compare how would the models perform against each type. Particularly, we perform experiments to answer the following research questions:

- **Experiment 1.** Is the knowledge extracted from a XGBoost model trained on abnormality patches useful to predict pathology of full mammogram images?
- **Experiment 2.** Is the knowledge extracted from a XGBoost model trained on full mammogram images useful to predict pathology of abnormality patches?
- **Experiment 3.** Which type of image would provide better features for pathology classification?
- **Experiment 4.** What is the XGBoost performance when trained on dataset B? What if we transfer knowledge and continue training in dataset A?
- **Experiment 5.** Is knowledge transfer with no fine-tuning useful for VGG16?
- **Experiment 6.** What is the VGG16 performance when trained from scratch with no knowledge transfer?
- **Experiment 7.** Is knowledge transfer with fine-tuning useful for VGG16?
- **Experiment 8.** What is the VGG16 performance when trained on dataset B? What if we transfer knowledge and continue training in dataset A?

Table 3 presents the experimental results for all the previous research questions. From Table 3 we observe that train XGBoost model on abnormality patches to predict pathology of full mammogram images (Experiment 1) is better than train XGBoost model on full mammogram images to predict pathology of abnormality patches (Experiment 2). Additionally, we observe that transfer learning provide negligible gains for XGBoost, since the AUC metric of 0.6829 in the Experiment 3 with dataset A (no transfer learning) is almost the same as AUC metric of 0.6849 in the Experiment 4 (with transfer learning). Moreover, we observe that abnormality-focused patch images impact negatively in XGBoost performance as the AUC score for Experiment 3 dataset B was 19.14% less accurate than dataset A, and 10.10% less accurate than dataset C. However, Experiment 4 shows that abnormality-focused images can be effectively used for transfer learning, since the knowledge learned by the pre-trained model that use these images (Experiment 3 dataset B) provides outperforming results when transferred to train dataset A.

Similarly to XGBoost, for VGG16 we observe that abnormality-focused patch images impact nega-

Table 3: Experimental results for XGBoost and VGG16.

Algorithm	Experiment	Dataset	AUC	Precision	Recall	F1-Score
XGBoost	1	-	0.5694	0.5260	0.5541	0.4755
	2	-	0.4207	0.5050	0.5308	0.3303
	3	A	0.6829	0.6411	0.6409	0.6410
		B	0.5522	0.5471	0.5516	0.5461
		C	0.6139	0.5780	0.5852	0.5780
	4	-	0.6849	0.6219	0.6243	0.6228
VGG16	5	A	0.6527	0.6022	0.5988	0.5905
		B	0.6151	0.5138	0.5833	0.4287
		C	0.6279	0.5472	0.5542	0.5442
	6	A	0.6233	0.5843	0.5838	0.5841
	7	A	0.6822	0.6405	0.6406	0.6405
		B	0.6207	0.5082	0.5679	0.4133
		C	0.6331	0.5598	0.5804	0.5506
	8	-	0.6527	0.6026	0.6014	0.5828

tively in performance, since the AUC score for Experiment 5 dataset B is 5.77% smaller than dataset A, and 2.04% smaller than dataset C. Additionally, Experiment 6 show that training network from scratch provide downgraded results, particularly a drop of 4.50% in AUC score when compared to the best result from Experiment 5. Moreover, Experiment 7 shows that transfer learning with fine-tuning impacts positively VGG16 models, particularly for dataset A, with an increase in AUC score of 4.52%. Finally, Experiment 8 shows that, differently from XGBoost, abnormality-focused images can not be effectively used for transfer learning, since the knowledge learned by the pre-trained model that use these images (Experiment 5 dataset B) provides inferior results when transferred to train dataset A (0.6527 of AUC in Experiment 8 compared to 0.6822 of AUC in Experiment 7).

In summary, both XGBoost and VGG16 performs better when trained with original full mammogram images, but XGBoost slightly outperforms VGG16 for classification of malignant tumors. For XGBoost, abnormality-focused images can be effectively used for transfer learning, but not for VGG16. Also, transfer learning with fine-tuning impacts positively VGG16, but provides negligible gains for XGBoost. Precision, recall, and F1-Score measures follow the same behavior than AUC metrics. Both XGBoost and VGG16 can effectively discriminate instances belonging to the benign class, but there is still room for improvement for malignant tumors classification.

7 CONCLUSION

In this article we compared the performance of XGBoost and VGG16 for breast cancer detection. Experiments with CBIS-DDSM dataset show that they performed similarly, achieving AUC scores of approximately 0.68. In addition, experimental results show that patch images did not contribute to performance. Moreover, XGBoost were able to identify more malignant samples than VGG16, finding a better balance between both classes.

A limitation of this work is the amount of cases in the CBIS-DDSM dataset. A larger well-annotated dataset would contribute to deeply train a CNN and further explore their ability to extract features from raw data. For future work, we intent to: i) perform experiments with other mammography screening datasets that can either be used individually or combined to increase the number of available cases; ii) perform image normalization and feature extraction to assist ML algorithms, since mammograms have noisy, and possibly annotations not relevant to the problem; iii) combine image datasets with textual image metadata and demographic information from patients; iv) use ensembles that can handle high-resolution images; v) perform experiments with datasets containing patients historical information to perform analysis of abnormalities growth over time.

ACKNOWLEDGEMENTS

The present work was carried out with the support of the Coordenação de Aperfeiçoamento de Pessoal de Nível Superior - Brazil (CAPES) - Financing Code 001. The authors thank the partial support of the CNPq (Brazilian National Council for Scientific and Technological Development), FAPEMIG (Foundation for Research and Scientific and Technological Development of Minas Gerais) and PUC Minas.

REFERENCES

Abiodun, O. I., Jantan, A., Omolara, A. E., Dada, K. V., Mohamed, N. A., and Arshad, H. (2018). State-of-the-art in artificial neural network applications: A survey. *Heliyon*, 4(11):e00938.

Bakator, M. and Radosav, D. (2018). Deep learning and medical diagnosis: A review of literature. *Multimodal Technologies and Interaction*, 2(3).

Chen, T. and Guestrin, C. (2016). XGBoost: A scalable tree boosting system. In *Proceedings of the 22nd ACM SIGKDD International Conference on Knowledge Discovery and Data Mining*, KDD'16, page 785–794.

Darby, S. C., Ewertz, M., McGale, P., Bennet, A. M., Blom-Goldman, U., Brønnum, D., Correa, C., Cutter, D., Gagliardi, G., Gigante, B., Jensen, M.-B., Nisbet, A., Peto, R., Rahimi, K., Taylor, C., and Hall, P. (2013). Risk of ischemic heart disease in women after radiotherapy for breast cancer. *New England Journal of Medicine*, 368(11):987–998.

DeSantis, C. E., Ma, J., Gaudet, M. M., Newman, L. A., Miller, K. D., Goding Sauer, A., Jemal, A., and Siegel, R. L. (2019). Breast cancer statistics. *CA: A Cancer Journal for Clinicians*, 69(6):438–451.

Lee, R., Gimenez, F., Hoogi, A., Miyake, K., Gorovoy, M., and Rubin, D. (2017). A curated mammography data set for use in computer-aided detection and diagnosis research. *Scientific Data*, 4:170177.

Li, H., Zhuang, S., ao Li, D., Zhao, J., and Ma, Y. (2019). Benign and malignant classification of mammogram images based on deep learning. *Biomedical Signal Processing and Control*, 51:347–354.

Liu, W., Wang, Z., Liu, X., Zeng, N., Liu, Y., and Alsaadi, F. E. (2017). A survey of deep neural network architectures and their applications. *Neurocomputing*, 234:11–26.

Løberg, M., Lousdal, M. L., Bretthauer, M., and Kalager, M. (2015). Benefits and harms of mammography screening. *Breast Cancer Research*, 17(1):63.

Loyola-González, O. (2019). Black-box vs. white-box: Understanding their advantages and weaknesses from a practical point of view. *IEEE Access*, 7:154096–154113.

Mohamed, A. A., Berg, W. A., Peng, H., Luo, Y., Jankowitz, R. C., and Wu, S. (2018). A deep learning method for classifying mammographic breast density categories. *Medical Physics*, 45(1):314–321.

Perre, A. C., Alexandre, L. A., and Freire, L. C. (2019). Lesion classification in mammograms using convolutional neural networks and transfer learning. *Computer Methods in Biomechanics and Biomedical Engineering: Imaging & Visualization*, 7(5-6):550–556.

Pouyanfar, S., Sadiq, S., Yan, Y., Tian, H., Tao, Y., Reyes, M. P., Shyu, M.-L., Chen, S.-C., and Iyengar, S. S. (2018). A survey on deep learning: Algorithms, techniques, and applications. *ACM Computing Surveys*, 51(5):92:1–92:36.

Ribli, D., Horváth, A., Unger, Z., Pollner, P., and Csabai, I. (2018). Detecting and classifying lesions in mammograms with deep learning. *Scientific Reports*, 8(1):4165.

Russakovsky, O., Deng, J., Su, H., Krause, J., Satheesh, S., Ma, S., Huang, Z., Karpathy, A., Khosla, A., Bernstein, M., Berg, A. C., and Fei-Fei, L. (2015). ImageNet Large Scale Visual Recognition Challenge. In *Proceedings of the International Journal of Computer Vision*, IJCV'15, pages 211–252.

Russell, S. and Norvig, P. (2009). *Artificial Intelligence: A Modern Approach*. Prentice Hall Press, Upper Saddle River, NJ, USA, 3rd edition.

Shen, D., Wu, G., and Suk, H.-I. (2017). Deep learning in medical image analysis. *Annual Review of Biomedical Engineering*, 19:221–248.

Simonyan, K. and Zisserman, A. (2014). Very deep convolutional networks for large-scale image recognition. *CoRR*, abs/1409.1556.

Sprague, B. L., Conant, E. F., Onega, T., Garcia, M. P., Beaber, E. F., Herschorn, S. D., Lehman, C. D., Tosteson, A. N. A., Lacson, R., Schnall, M. D., Kontos, D., Haas, J. S., Weaver, D. L., Barlow, W. E., and Consortium, P. R. O. S. P. R. (2016). Variation in mammographic breast density assessments among radiologists in clinical practice: A multicenter observational study. *Annals of Internal Medicine*, 165(7):457–464.

Tan, C., Sun, F., Kong, T., Zhang, W., Yang, C., and Liu, C. (2018). A survey on deep transfer learning. In Kůrková, V., Manolopoulos, Y., Hammer, B., Iliadis, L., and Maglogiannis, I., editors, *Proceedings of the 27th International Conference on Artificial Neural Networks and Machine Learning*, ICANN'18, pages 270–279.

Vadivel, A. and Surendiran, B. (2013). A fuzzy rule-based approach for characterization of mammogram masses into BI-RADS shape categories. *Computers in Biology and Medicine*, 43(4):259 – 267.

Vibha, L., Harshavardhan, G. M., Pranaw, K., Shenoy, P. D., Venugopal, K. R., and Patnaik, L. M. (2006). Classification of mammograms using decision trees. In *Proceedings of the 10th International Database Engineering and Applications Symposium*, IDEAS'06, pages 263–266.

Wu, N., Geras, K. J., Shen, Y., Su, J., Kim, S. G., Kim, E., Wolfson, S., Moy, L., and Cho, K. (2018). Breast density classification with deep convolutional neural networks. In *Proceedings of the IEEE International Conference on Acoustics, Speech and Signal Processing*, ICASSP'18, pages 6682–6686.